Multiaxial Fatigue Modelling and Some Simple Approximations

A. Fatemi and N. Shamsaei

Mechanical, Industrial and Manufacturing Engineering, The University of Toledo, 2801 West Bancroft Street, Toledo, Ohio 43606, USA, afatemi@eng.utoledo.edu

ABSTRACT. *A brief overview of some important issues in multiaxial fatigue and life estimation is presented. While not intended to be comprehensive, these are a relatively broad range of issues which are commonly encountered when dealing with multiaxial fatigue. They include damage mechanisms, non-proportional hardening and constitutive behavior, damage parameters and life estimation, variable amplitude loading, cycle counting, damage accumulation, and mixed-mode crack growth. Some simple approximations in capturing some of these effects in multiaxial life estimations are also presented.*

INTRODUCTION

Multiaxial loads, which can be in-phase (proportional) or out-of-phase (non-proportional), are common for many components and structures. Even under uniaxial loads multiaxial stresses often exist, although typically in-phase, for example due to geometric constraints at notches. Such multiaxial loads and stress states are frequently encountered in many industries, including automotive, aerospace, and power generation, among others.

The earliest works on multiaxial stress states, although under monotonic loading, relate to classical yield theories of Lame and Tresca in the late 19th century and von Mises in the early 20th century. While the first combined load testing is attributed to Lanza in 1886 [1], the first systematic study of multiaxial fatigue was conducted by Gough and Pollard in 1930's [2]. The bending-torsion data generated from the study of Gough and Pollard provided the basis for the models later proposed by Gough [3], Sines [4], and Findley [5] in the 1950's. Much of the early multiaxial fatigue work, however, related to high cycle fatigue and S-N analysis, where plastic strain is typically small or negligible.

Since these early works, much additional experimental as well as theoretical works on the challenging problem of multiaxial fatigue have been accomplished, particularly in the last four decades, with the advent of accurate multiaxial fatigue testing equipment. A series of international conferences and symposia have been dedicated to this topic in the last 30 years, including those in San Francisco-USA in 1982, Sheffield-UK in 1985, Stuttgart-Germany in 1989, San Diego-USA in 1991, St. German-en-Layne-France in

1994, Denver-USA in 1995, Cracow-Poland in 1997, Lisbon-Portugal in 2001, Berlin-Germany in 2004, and Sheffield-UK in 2007.

The results from these conferences and symposia have been published in proceedings, and some have been published as ASTM Special Technical Publications (STP 853, STP 1191, STP 1280, and STP 1387). SAE Fatigue Design and Evaluation Committee also had a multiaxial fatigue testing and analysis program in the 1980's and the 1990's, the results of which were published as SAE Advances in Engineering series (AE 14 and AE 28). A multiaxial fatigue book by Socie and Marquis [6] provides working knowledge of multiaxial fatigue damage processes and life estimation models, including illustrative examples.

The large amount of experimental data generated and research performed over the last four decades has significantly advanced the understanding of the complex issue of multiaxial fatigue. However, as this challenging problem remains elusive, and due to its practical application significance, much additional research and development work is still needed for accurate and reliable evaluation of multiaxial fatigue design, life estimation, and failure assessment.

This paper is not intended to be a review paper, but rather, an overview sort of paper, where several important issues related to multiaxial fatigue are discussed. These include brief discussions of: 1) damage mechanisms, as they provide the basis for critical plane life prediction approaches, 2) non-proportional hardening and constitutive behavior, since they can significantly affect fatigue behavior, 3) damage parameters and life estimation, as they are key ingredients of any life assessment methodology, 4) variable amplitude loading, cycle counting, and damage accumulation, due to their significant implications related to service loadings of many structures and components, and 5) mixed-mode crack growth, as it can constitute a significant portion of the total fatigue life. Some simple approximations for capturing some of these effects in multiaxial life estimation are also provided.

Although the scope of this paper is relatively broad, it is by no means comprehensive, as some other important effects such as notch behavior and elevated temperatures are not included. It should also be mentioned that much of the data and many of the models presented are based on or influenced by the author and his collaborators works in this area, and therefore, admittedly biased. Therefore, as this is not a literature survey or review paper, many other works in this area, although significant, are not presented.

DAMAGE MECHANISMS

Fatigue life generally consists of crack nucleation and crack growth. In ductile behaving materials, cracks typically nucleate along slip systems, which are aligned with the maximum shear planes. In brittle behaving materials, cracks often nucleate directly at discontinuities, such as inclusions and voids, although they can also nucleate in shear. Once cracks nucleate, their growth can be divided in two stages, stage I associated with micro-crack growth (i.e. early growth) along maximum shear planes, and stage II

associated with crack growth along maximum tensile stress plane. Micro-crack growth life of ductile-behaving materials is typically dominated by stage I growth, while crack growth life of brittle-behaving materials is typically dominated by stage II growth.

Systematic investigation of cracking behavior under multiaxial loading by several investigators, including Socie and co-workers [7, 8] and Brown and Miller [9, 10], indicated that cracks nucleate and grow on preferred planes rather than with random orientation. The preferred orientation depends on the material and the state of loading. The preferred orientation of crack plane nucleation and growth has also been observed for non-metallic systems, such as in elastomers [11] with very different material structure than metals (i.e. polymer chains).

Examples of preferred crack plane nucleation and growth are shown in Fig. 1. Figure 1(a) shows a large number of cracks in normalized medium carbon steel under in-phase axial-torsion loading, where all the cracks are oriented along the maximum shear plane. Figure 1(b) shows multiple cracks in natural rubber under 90º out-of-phase axial-torsion loading, where they are all along the same preferred orientation. These cracks continue to grow along the same direction with increasing number of cycles.

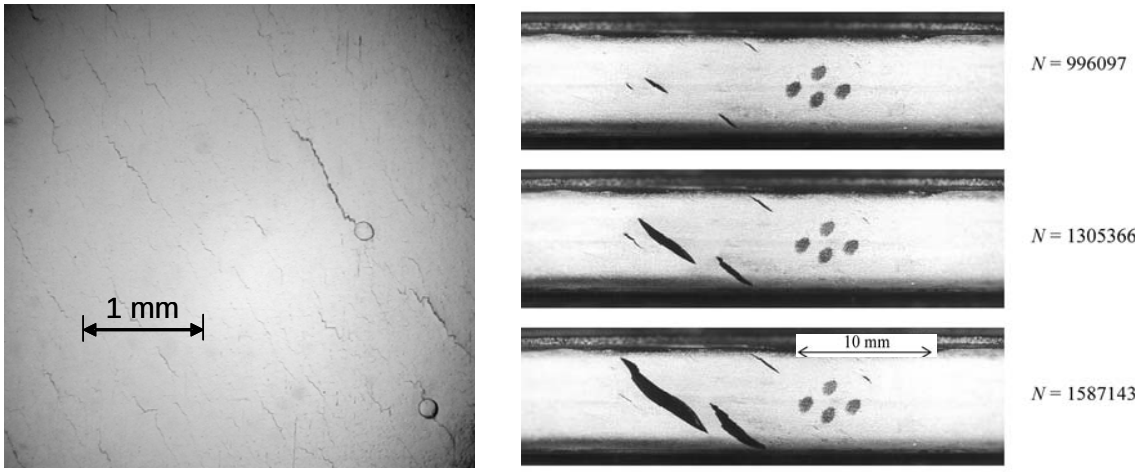

Figure 1. Preferred cracking orientations observed for (a) 1050 normalized steel under in-phase axial-torsion loading, and (b) natural rubber under 90º out-of-phase axial-torsion loading.

These observations have provided the physical basis for critical plane approaches to multiaxial fatigue. These approaches, which reflect the material damage mechanism, are based on either maximum shear failure plane, or maximum principal strain or stress failure plane. For the former case, the primary fatigue damage driving parameter is shear strain or stress, while for the latter case the primary damage driving parameter is the maximum principal stress or strain. For shear cracking mechanism materials, the stress normal to the cracking plane can have a secondary influence. This is because

cracks typically grow in a zigzag or irregularly shaped manner at the microscopic scale, as can be observed by close examination of the cracks in Fig. 1(a). A tensile normal stress opens the crack, reducing crack closure, and resulting in decreased fatigue life. In contrast, a compressive normal stress closes the crack, increasing crack closure and resulting in increased fatigue life. Figure 2 shows schematic representation of shear and tensile cracking mechanisms of an irregularly shaped crack.

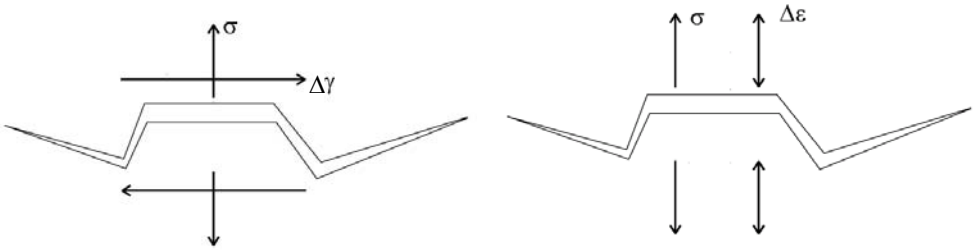

(a) (b)

Figure 2. Cracking mechanism for shear (a) and tensile (b) damage material [6].

NON-PROPORTIONAL HARDENING AND CONSTITUTIVE MODELLING

The principal directions of cyclic loading remain fixed in proportional multiaxial loading, whereas principal axes rotate in time for non-proportional multiaxial loading. Some materials exhibit strain hardening due to the non-proportionality of cyclic loading. This phenomenon was first observed by Taira et al. [12] and later explained by Lamba and Sidebottom [13] and Kanazawa et al. [14]. The additional hardening is attributed to the change in crystallographic slip planes due to the rotation of maximum shear plane and intersection of these planes under non-proportional loading.

The level of non-proportional cyclic hardening depends on the shape, sequence, and amplitude of the load path, as well as the microstructure of the material. Figure 3 shows cyclic deformation behavior of two materials under proportional (in-phase) and non-proportional (90º out-of-phase) loadings. While the Ti alloy Ti-6.5Al-3.4Mo exhibits the same behavior under the two loadings [15], the 304L stainless steel exhibits significant additional hardening under non-proportional loading [16].

The maximum possible strain hardening usually results from 90º out-of-phase loading. Sensitivity of a material to non-proportional cyclic loading is commonly determined by non-proportional cyclic hardening coefficient, α , defined as:

$$\alpha = \frac{\overline{\sigma}_{OP}}{\overline{\sigma}_{IP}} - 1 \tag{1}$$

where $\overline{\sigma}_{OP}$ is 90° out-of-phase equivalent stress amplitude and $\overline{\sigma}_{IP}$ is in-phase equivalent stress amplitude at the same strain amplitude level.

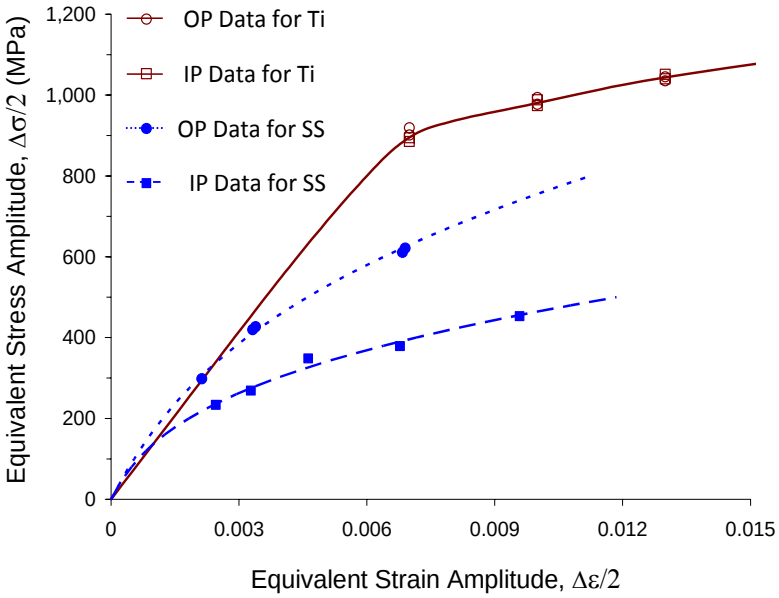

Figure 3. Comparison of in-phase (IP) and 90° out-of-phase (OP) equivalent stress-strain data for Ti-6.5Al-3.4Mo (Ti) and 304L stainless steel (SS).

Shamsaei and Fatemi [16] observed that cyclic hardening materials also exhibit non-proportional hardening under non-proportional loading, whereas cyclic softening materials do not typically display additional cyclic hardening. As both cyclic hardening and non-proportional hardening are associated with the stacking fault energy, they related the non-proportional cyclic hardening coefficient, α, to uniaxial cyclic deformation properties K' and n', and proposed the following empirical relation:

$$\alpha = 1.6\left(\frac{K}{K'}\right)^{2}\left(\frac{\Delta\varepsilon}{2}\right)^{2(n-n')} - 3.8\left(\frac{K}{K'}\right)\left(\frac{\Delta\varepsilon}{2}\right)^{(n-n')} + 2.2 \qquad (2)$$

where K, K', n, and n' are uniaxial strength coefficient, cyclic strength coefficient, strain hardening exponent, and cyclic strain hardening exponent, respectively.

Experimental non-proportional cyclic hardening coefficients are compared with the predicted values based on Eq. 2 for a wide variety of metallic materials in Fig. 4. This figure indicates very good predictions. Therefore, this relation provides a simple approximation for the non-proportional cyclic hardening coefficient based on commonly available or easily obtainable uniaxial cyclic deformation material properties.

In general, there are two methodologies for estimation of stress response under general multiaxial loading; empirical formulations and constitutive models. Empirical models, such as in [14], relate the stress response of non-proportional loading directly to the strain path. Although these empirical models are simple, they may result in significant errors in estimation of stress response and, therefore, fatigue life [17].

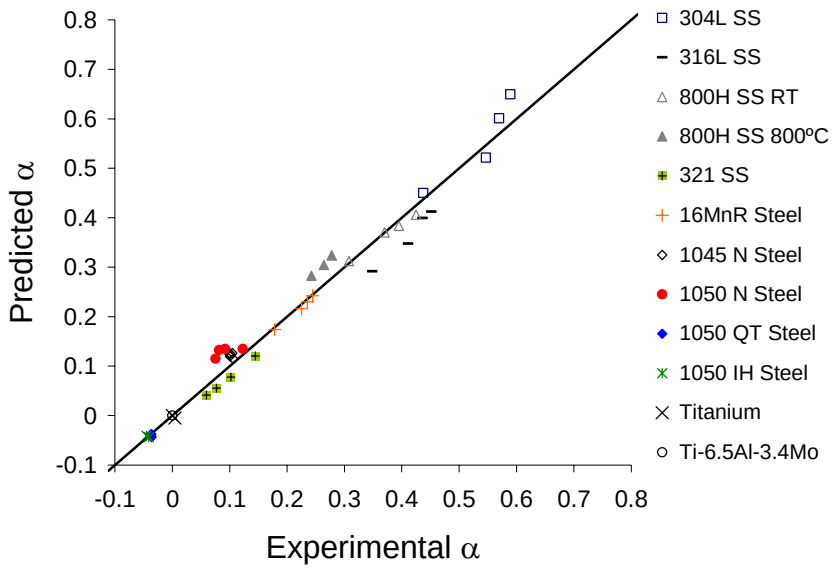

Figure 4. Comparison of experimental and predicted values of non-proportional cyclic hardening coefficient, α, based on Eq. 2 [16].

Plasticity models which develop constitutive behavior based on continuum mechanics usually result in much better predictions of stress response for complex loading, as compared to empirical models. The Armstrong-Frederick incremental plasticity model [18] has been shown in several studies, such as [19, 20], as a proper basis for modeling various features of material behavior such as ratcheting, non-proportional hardening, and cyclic softening and hardening. This model considers the movement of the yield surface in deviatoric stress space by a nonlinear kinematic hardening rule, taking into account the strain memory effect by a recovery term.

Non-proportional cyclic hardening in constitutive models is taken into account by a non-proportionality parameter. Tanaka's non-proportionality parameter [21] has been reported to provide satisfactory predictions for a variety of materials under various non-proportional loading conditions, such as in [17, 21, 22]. This parameter is a function of the normalized plastic strain rate vector and the internal microstructure of material is represented by a fourth rank tensor in a 5-D plastic strain vector space.

Shamsaei et al. [17] used Tanaka's non-proportionality parameter coupled with a simplified form of the Armstrong-Frederick incremental plasticity model which only requires five material constants (E, G, K', n', α) to predict stress response for 304L stainless steel under several axial-torsion strain paths. In addition to in-phase and 90º out-of-phase strain paths, some star shape strain paths were also used, shown on the left side of Fig. 5. One strain path consists of 360 proportional fully-reversed axial-torsion cycles with 1° increments starting from the pure axial cycle in $\gamma/\sqrt{3}$-ε strain space. Another strain path also includes 360 proportional fully-reversed axial-torsion cycles, but applied in a random sequence. Therefore, the two paths are identical, except for the straining sequence. 304L stainless steel exhibited significant sensitivity to the straining

sequence. In-phase loading with gradual change in strain direction (i.e. 1° increments), which activates the slip systems gradually but in all directions, resulted in some non-proportional hardening, as compared with in-phase loading. Star shape strain path with random sequence resulted in significant non-proportional hardening and similar to 90° out-of-phase loading due to cross hardening and severe interaction of the slip systems.

Tanaka's non-proportionality parameter coupled with the simplified form of the Armstrong-Frederick plasticity model resulted in stress response predictions within 12% of experimental values for all the strain paths employed [23]. Kanazawa et al. empirical non-proportionality formulation, however, which considers the load non-proportionality as a factor of ellipticity of the circumscribed boundary around the strain path in the $\gamma/2$-ε plot, predicts identical stress response for the 90º out-of-phase and the star shape strain paths, regardless of straining sequence. This significantly over-estimates the stress for star path straining with gradual change in direction, as observed from Fig. 5.

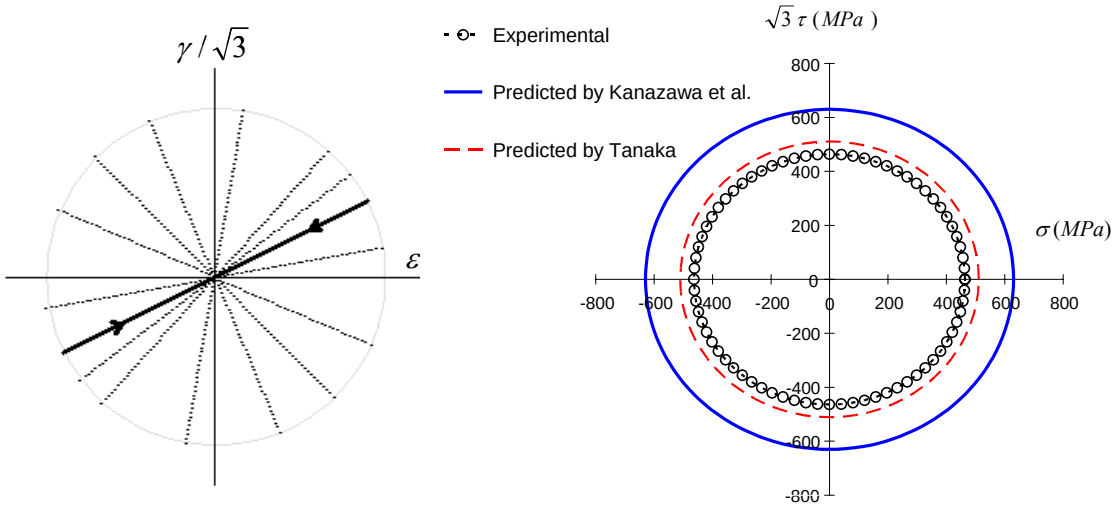

Figure 5. Experimental and predicted stress boundary for star shape path with gradual change in strain direction at 0.7% effective strain amplitude for 304L stainless steel [17].

DAMAGE PARAMETERS AND LIFE ESTIMATION

Classical yield criteria, such as von Mises distortion energy criterion, are commonly extended to multiaxial fatigue life estimations. Although these criteria may work for in-phase or proportional loading, they often under-estimate the typically observed shorter lives for out-of-phase or non-proportional loading. For example, for 90º out-of-phase sinusoidal axial-torsion loading with axial stress related to torsion stress by $\sqrt{3}$, von Mises equivalent stress remains constant during the loading cycle. This implies infinite life, regardless of the cyclic stress amplitudes. Therefore, such criteria are not generally appropriate for out-of-phase or non-proportional loading.

The shorter life of non-proportional loading is often attributed to non-proportional hardening. However, materials without this hardening also typically exhibit shorter life under such loading. Figure 6 shows comparison of fatigue lives for in-phase and 90º out-of-phase loading for Ti-6.5Al-3.4Mo [15] and 1050 normalized (N) steel [24]. The Ti alloy is a material without non-proportional hardening (see Fig. 3), while 1050 N steel exhibits about 10 to 15% non-proportional cyclic hardening. As can be seen from Fig. 6, both materials show shorter life under out-of-phase loading at the same equivalent strain as in-phase loading, although the difference is larger for the 1050 N steel. von Mises criterion predicts the same fatigue damage for both loadings and does not correlate the two sets of data for either material, as observed in Fig. 6.

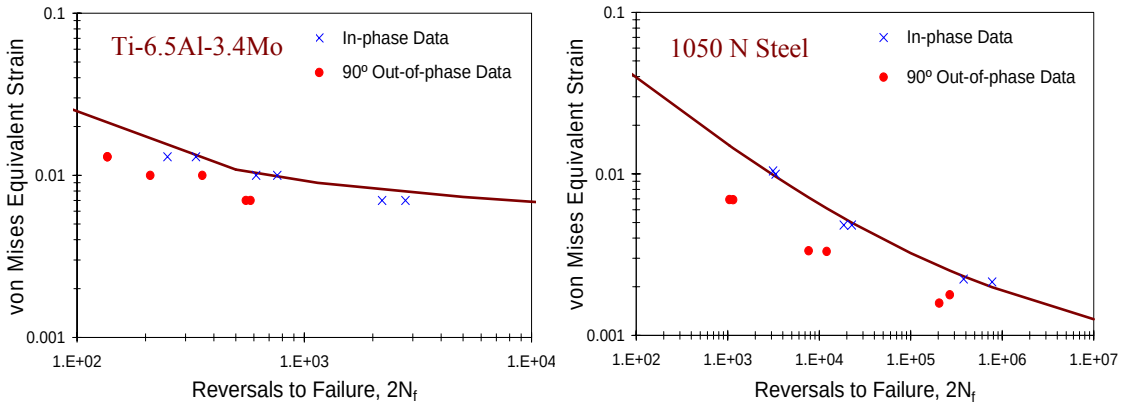

Figure 6. Fatigue data correlations by von Mises criterion for Ti-6.5Al-3.4Mo and 1050 normalized (N) steel.

Damage observations such as those presented in Fig. 1, and much work in the last 30 years suggests critical plane approaches are most reliable and robust for multiaxial fatigue life estimations. As discussed previously, these approaches reflect the physical nature of fatigue damage process. They consider specific plane(s) with maximum fatigue damage as the critical plane and are, therefore, also able to predict damage (i.e. crack) orientation. Critical plane approaches have been found to be applicable to both proportional and non-proportional loading conditions, and their applicability is not limited to metallic materials. For example, for elastomers, it has been shown that critical plane damage parameters are more accurate than scalar criteria such as von Mises, or the commonly used strain energy density criterion (SED), commonly used for elastomeric material life estimations [25, 26].

Critical plane approaches are typically based on either the maximum shear plane or the maximum principal plane failure mode, as presented in Fig. 2. They can be classified as stress-based, strain-based, and strain-stress-based or energy-based models. Stress-based critical plane models, such as Findley [27] model, may work well for high cycle fatigue (HCF), where plastic deformation is small or negligible. However, in many encountered fatigue problems, cyclic plastic deformation plays an important role

in the damage process. This includes low cycle fatigue (LCF), notched components, and variable amplitude service loads containing overload cycles.

Strain-based critical plane models, such as Brown and Miller [10] model, are only based on strain terms. Although these models may apply to both low and high cycle fatigue, they cannot reflect constitutive behavior of the material. Therefore, effects of phenomena such as non-proportional cyclic hardening which can have a significant effect on fatigue life cannot be taken into account. In addition, such criteria typically predict two orthogonal critical planes, since both planes have the same shear and normal strains. However, cracking is usually observed on one preferred plane. For example, Fig. 1(a) shows that while many cracks exist, they are all on a single plane, rather than on two orthogonal planes. Thus, strain alone is not sufficient to identify the preferred critical plane and quantify fatigue damage.

Critical plane models with both stress and strain are, therefore, the most appropriate for general applicability to both LCF and HCF, and with the ability to capture material constitutive response under non-proportional loading. Strain-stress-based critical plane models typically include a driving strain parameter and a secondary influencing stress parameter. Fatemi-Socie (FS) parameter [28] for shear failure mode materials and Smith-Watson-Topper parameter [29] for tensile failure mode materials are examples of such critical plane models, with the corresponding damage mechanisms shown in Fig. 2.

The FS damage parameter is expressed as a function of the maximum shear strain amplitude, $\Delta\gamma_{\max}/2$, and the maximum normal stress acting on the maximum shear strain plane over the cycle, $\sigma_{n,\max}$, as:

$$\frac{\Delta\gamma_{\max}}{2}\left(1+k\frac{\sigma_{n,\max}}{\sigma_y}\right) \tag{3}$$

where σ_y is the material monotonic yield strength, and k is a material constant which can be found by fitting uniaxial fatigue data to torsion fatigue data. A distinct feature of this parameter is the coupling between the shear strain and the normal stress terms. Due to this coupling, shear strain alternation must be present for the normal stress term to cause fatigue damage. This prevents the normal stress term from contributing to fatigue damage, if the loading is not alternating (i.e. static loading). Damage parameters without this coupling can incorrectly predict fatigue damage from static loads. Multiaxial fatigue data correlations and life estimations based on this parameter for a broad range of loadings and materials have been shown over the last two decades.

An example of damage distribution with plane orientation for in-phase and 90° out-of-phase axial-torsion loading with the same effective strain for Ti-6.5Al-3.4Mo [15] based on the FS parameter is shown in Fig. 7. A higher normal stress on the maximum shear plane for out-of-phase loading results in a higher damage value, as can be seen from Fig. 7, with the maximum damage on the 0° plane. Therefore, a shorter fatigue life is calculated as compared to in-phase loading, which corresponds with the experimental results (see Fig. 6). This is in spite of the fact that this Ti alloy does not exhibit non-

proportional hardening under out-of-phase loading (see Fig. 3). For a material with non-proportional hardening, the normal stress term in Eq. 3 increases to a higher value, as compared to a material without this hardening. As Fig. 7 indicates, von Mises criterion predicts the same damage for in-phase and 90° out-of-phase loadings, and on all planes.

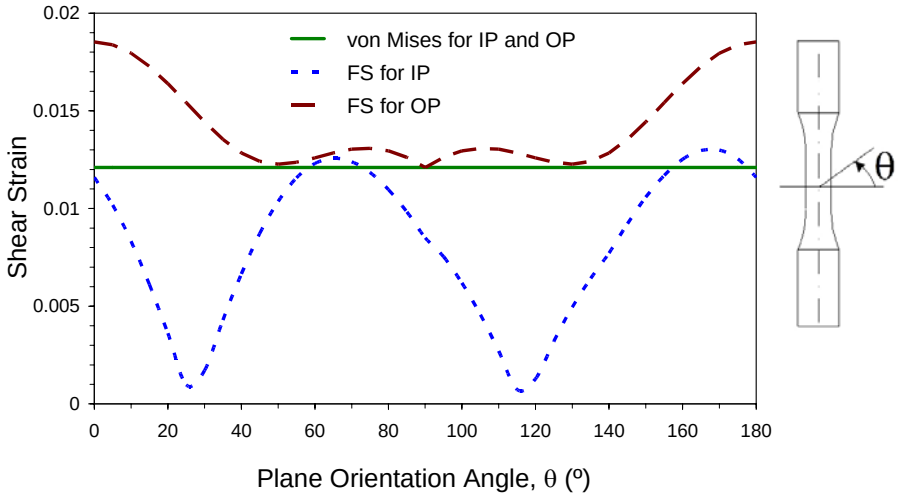

Figure 7. Variation of von Mises and FS damage parameters with plane orientation for $\bar{\varepsilon}_a$ = 0.7% of Ti-6.5Al-3.4Mo for in-phase (IP) and 90° out-of-phase (OP) axial-torsion loadings.

Mean and/or residual stresses can also have a significant effect on fatigue behaviour. In multiaxial fatigue, the direction of the mean stress(s) with respect to the damage plane (critical plane) is an important consideration. For example, for a shear failure mode material, a tensile mean stress normal to the damage plane in Fig. 2(a) opens the crack, facilitating crack growth, resulting in shorter life. A compressive mean stress would have the opposite effect. However, a normal mean or static stress parallel to the shear critical plane in Fig. 2(a) may not have any influence on fatigue life. Therefore, the effect of the mean stress also depends on the material failure mode. Experimental evidence for these observations and discussions of mean or static normal and shear stresses are provided in [6, 30]. The effect of a normal stress on the critical plane in the FS damage parameter is taken into account through the normal stress term, where the maximum normal stress $\sigma_{n,\max}$ is composed of alternating and mean stress components.

A difficulty in life estimation is often lack of needed material fatigue properties. To enable calculation of multiaxial fatigue life in the absence of any fatigue data, a simple approximation for steels based on hardness is presented in [24]. This approximation combines the FS parameter with the Roessle-Fatemi hardness method [31], given by:

$$\frac{\Delta\gamma_{\max}}{2}\left(1+k\frac{\sigma_{n,\max}}{\sigma_y}\right)=\left[A(2N_f)^{-0.09}+B(2N_f)^{-0.56}\right]\left[1+kC(2N_f)^{-0.09}\right] \quad (4)$$

where $k \approx 1$ and parameters A, B, and C are given in terms of Brinell hardness (HB) as:

$$A = \frac{5.53(HB) + 293}{200{,}000}, \quad B = \frac{0.48(HB)^2 - 731(HB) + 286{,}500}{200{,}000}, \quad C = \frac{1}{0.0022(HB) + 0.382}$$

If not available, yield strength (σ_y) can also be estimated as a function of hardness [24].

Estimated fatigue lives based on Eq. 4 and only hardness as material property for several steels are compared with experimental lives in Fig. 8. This includes 1050 steel in normalized (N), quenched and tempered (QT), and induction-hardened (IH) conditions, two stainless steels, and Inconel 718 under a wide variety of loadings including axial-torsion and tension-tension, in-phase and out-of-phase, and with or without mean stress. In Fig. 8, 80% and 93% of the data fall within scatter bands of 3 and 5, respectively.

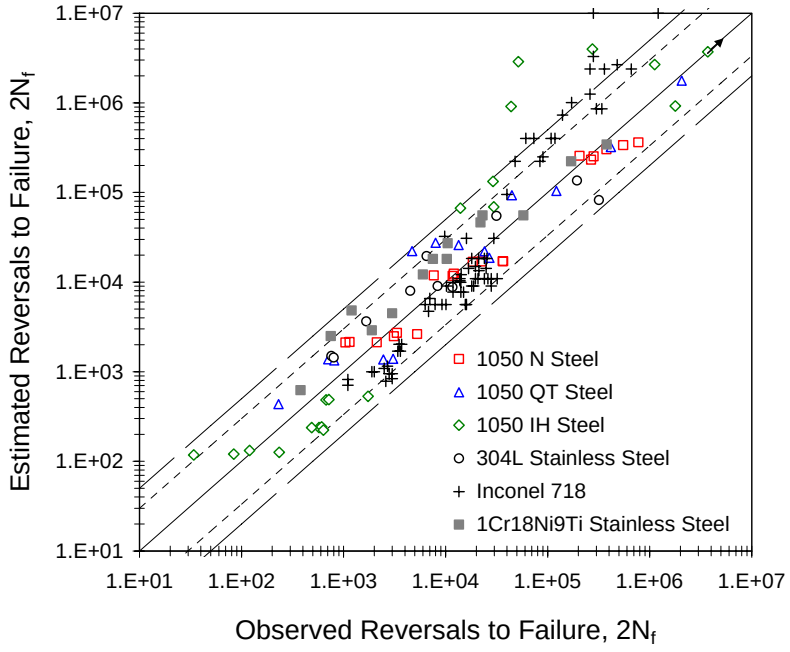

Figure 8. Comparison of observed and estimated fatigue lives based on hardness for different materials under multiaxial loading conditions.

VARIABLE AMPLITUDE LOADING, CYCLE COUNTING, AND DAMAGE ACCUMULATION

To evaluate fatigue life under variable amplitude multiaxial loading, three components are essential: 1) a cycle counting method to identify cycles in the load history, 2) a multiaxial fatigue damage parameter to evaluate fatigue damage caused by each identified cycle, and 3) a cumulative damage rule to sum damage from all the counted

cycles. Since a discussion of multiaxial damage parameters was already presented, only cumulative damage and cycle counting are discussed in this section.

To compute the accumulated fatigue damage in variable amplitude loading, many nonlinear cumulative damage rules have been proposed. These nonlinear rules have been intended to address some of the shortcomings of the linear damage rule (LDR), such as load sequence and deformation history effects. However, LDR remains as the simplest and most commonly used cumulative damage rule [32].

Some of the shortcomings attributed to LDR in computing fatigue damage in the literature are not necessarily due to LDR, but due to the use of an unsuitable damage parameter. For example, even in uniaxial variable amplitude loading of strong deformation history dependent materials such as stainless steel, it has been shown that LDR works very well if a damage parameter including both stress and strain terms is used to quantify damage from each cycle, rather than the commonly used S-N or strain-life curves [33]. This approach accounts for the deformation history dependence (i.e. constitutive response) of fatigue damage in each cycle damage calculation. However, while this approach addresses the deformation history dependence aspect in load sequence effects, it does not account for load amplitude dependence of load sequence effects which also usually exists. High amplitude cycles followed by low amplitude cycles are usually more damaging than the reverse sequence, even for materials without constitutive behavior sensitivity to load sequence, such as some aluminum alloys [33].

In multiaxial fatigue, load path alteration can also affect fatigue life. For example, torsion followed by tension has been found to be more damaging than tension followed by torsion [34, 35]. This has been explained [6] by torsion cycles nucleating small cracks on planes where subsequent tensile cycles can lead to their growth, while tensile cycles do not nucleate cracks on planes which can grow by torsion cycles. In LCF of Ti and its alloy presented in Fig. 9(a), however, tension-torsion sequence (B1 block) was observed to be slightly more damaging than torsion-tension sequence (B2 block) [15].

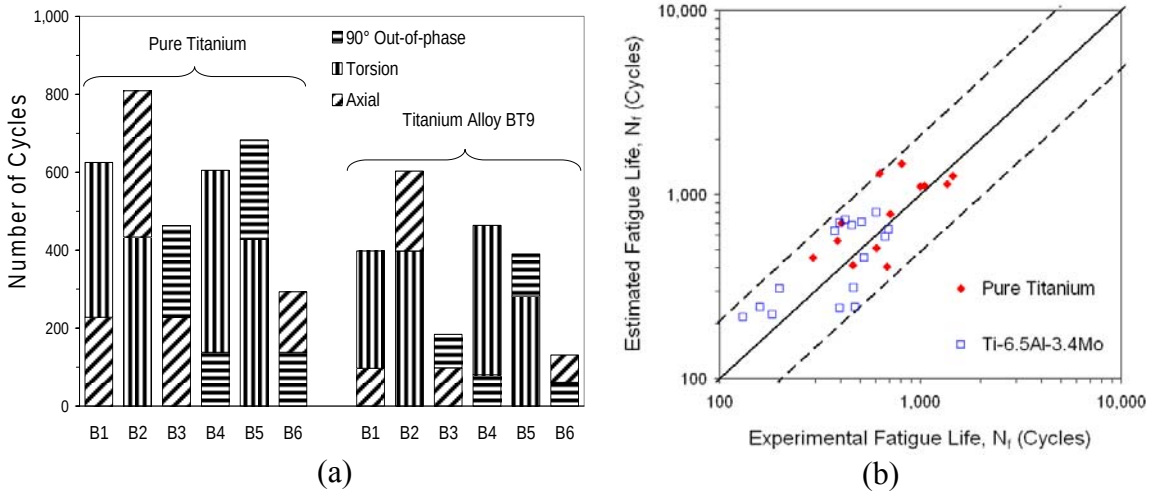

Figure 9. (a) Observed fatigue lives for several strain block loadings of Ti and its alloy. (b) Comparison of observed and calculated fatigue lives by LDR and FS parameter [15].

In addition to axial (i.e. tension)-torsion and torsion-axial sequences, Fig. 9(a) also includes sequences of axial or torsion with 90° out-of-phase straining. Each part of the sequence for each material in this figure has identical equivalent strain amplitude (0.9% for Ti and 1% for its alloy) and all strain blocks are fully-reversed (i.e. no mean stress). As seen from Fig. 9(a), shorter fatigue lives are observed by 90° out-of-phase loading followed by axial loading (B6 strain block), as compared to axial loading followed by 90° out-of-phase loading (B3 strain block). In addition, 90° out-of-phase followed by axial loading (B6 strain block) is more damaging than 90° out-of-phase followed by torsion loading (B4 strain block). It should be noted that as Ti and its alloy are not sensitive to non-proportional hardening (see Fig. 3), this is not a factor in the observed differences, or their explanations.

An important factor to consider when comparing the damage from each segment of the strain block is the parameter used for damage evaluation. Although each of the axial, torsion, and 90° out-of-phase segments of each block for each material in Fig. 9(a) has identical equivalent strain amplitude, the damage caused by each type of cycle is not the same. This is clearly observed from Fig. 10, where the damage value of each type of load in terms of the FS parameter is shown. The 90° out-of-phase loading causes a higher damage value than either axial or torsion loading. Placing 90° out-of-phase cycles at the beginning of a sequence (i.e. high-low loading) is, therefore, more damaging than placing them at the end of a sequence (i.e. low-high loading). This can explain the shorter live of the B6 strain block, as compared with the B3 strain block. Once small cracks nucleate under 90° out-of-phase cycles on or near 0° plane (see Fig. 10), they can then grow faster under subsequent tensile cycles than under subsequent torsion cycles. This can explain the shorter lives of the B6 block, as compared with the B4 block.

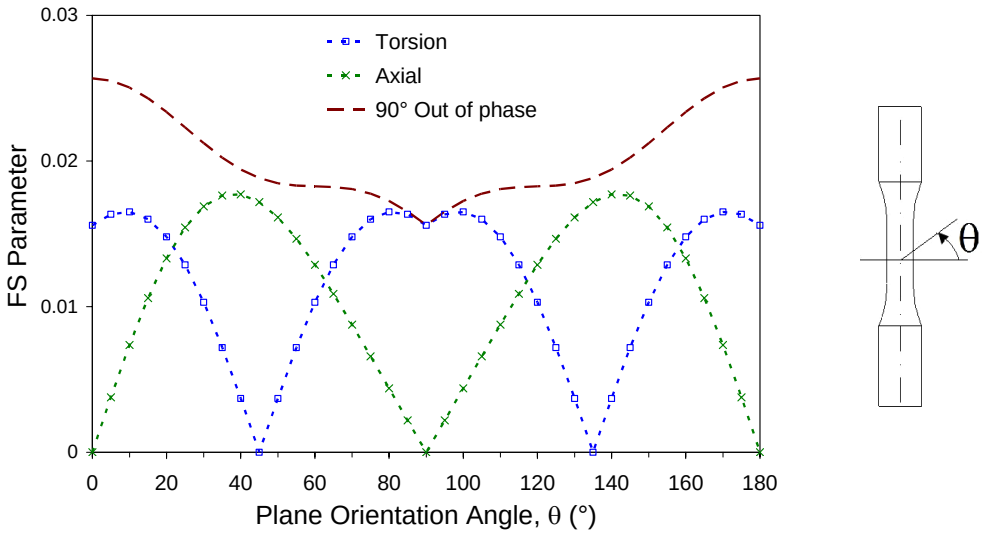

Figure 10. Variation of the FS damage parameter with plane orientation for axial, torsion, and 90° out-of-phase loadings of Ti at $\bar{\varepsilon}_a = 0.9\%$ [15].

Comparison of observed fatigue lives with predicted lives using LDR and FS parameter for various block loadings of Ti and its alloy are presented in Fig. 9(b). This figure includes the loading blocks from Fig. 9(a), as well as other blocks with several segments of axial, torsion, and 90° out-of-phase strain paths with the same equivalent strain, with each block repeated to failure [15]. To evaluate fatigue life, distribution of the damage parameter for each segment of loading was considered on different planes. Cumulative damage on each plane was then evaluated using LDR as the sum of damage caused by each segment of the load block. The plane with the greatest value of damage was then chosen as the critical plane and fatigue life was calculated for this plane. Figure 9(b) indicates the estimated fatigue lives to be within a factor of 2 of the experimental lives for both materials. Therefore, in spite of the fact that LDR does not account for some of the load sequence and load path alteration effects discussed with reference to the load blocks in Fig. 9(a), it still results in reasonable life estimates. Experimental results have also confirmed applicability of LDR for estimating fatigue life of elastomers under variable amplitude multiaxial loading [36].

In the case of general variable amplitude multiaxial loading, a cycle counting method is also required to identify different cycles within the load block. There are only a few proposals in the literature for cycle counting under multiaxial loading histories based on critical plane approaches. Bannantine and Socie [37] proposed a method based on the extension of critical plane concept and rainflow cycle counting on the strain history, as the main channel, mapped on the candidate planes within the material to determine the critical plane. In this method, rainflow cycle counting is performed on the shear strain history for shear failure mode materials, and on the normal strain history for tensile failure mode materials. Other components of the damage parameter (i.e. auxiliary channels), such as the maximum normal stress for FS parameter, are then determined for each counted cycle or reversal.

Wang and Brown [38] also proposed a cycle counting method based on a modified equivalent strain theory. To overcome the sign problem in the von Mises equivalent strain and to be able to count out-of-phase cycles, they proposed a modified strain history by assigning a turning point at the greatest value of the equivalent strain. This method counts reversals and then discards them from the strain history. A new turning point is then defined and the process continues until all reversals are counted.

Development of a reliable and robust cycle counting method for variable amplitude multiaxial loading remains a challenging problem. Related to this issue is the interaction between the components of the damage parameter, for example shear strain amplitude and maximum normal stress in FS parameter, for a counted cycle. Additional work is still needed to fully understand variable amplitude multiaxial loading effects in complex service load histories.

MIXED-MODE CRACK GROWTH

Once micro-cracks nucleate, they often coalesce to form a dominant macro-crack, although still small in size (typically on the order of 1 mm). In some applications, a

considerable portion of the total fatigue life is spent in macro-crack growth. Under multiaxial loads or stress states, the macro-crack can grow under mixed-mode loading conditions. As the crack often changes direction during its growth under mixed-mode loadings, both crack growth rate and crack growth direction are of important in such applications [39]. In plate-type geometries, although cracks may form under mix-mode loading, they often turn into a mode I macro-crack after their early micro-crack crack growth period. Also, short or small cracks often exhibit different crack growth behaviour than long cracks and the difference is usually attributed to differences in plasticity-induced and roughness-induced closure mechanisms.

Several criteria have been used to predict crack growth direction under mixed-mode loading conditions. Maximum tangential stress (MTS) [40] and minimum strain energy density [41] criteria have been widely used because of their simplicity and support by experimental observations. According to the MTS criterion, the crack extends in a direction corresponding to the maximum tangential stress. According to the minimum strain energy density criterion, the crack grows in a direction along which the strain energy density factor reaches a minimum value.

To correlate fatigue crack growth rates under mixed-mode loading, equivalent strain and equivalent stress intensity factors have been used. A Paris-type equation is then used to calculate crack growth life. An equivalent strain-based intensity factor based on Eq. 3 is given as [42]:

$$\Delta K_{CPA} = G\,\Delta\gamma_{\max}\left(1 + k\frac{\sigma_{n,\max}}{\sigma_y}\right)\sqrt{\pi c} \tag{5}$$

where c is surface crack half-length. This parameter was shown to correlate small crack growth rate data for a wide variety of loading conditions of tubular specimens of 1045 N steel and Inconel 718 [42]. The loadings included axial, torsion, proportional and non-proportional axial-torsion with and without mean stress, and biaxial tension.

An equivalent stress intensity factor for mixed-mode loading based on the assumption that a fatigue crack grows when the sum of the absolute values of the crack tip displacements in a plastic strip reaches a critical value is expressed by [43]:

$$\Delta K_{eq} = \left[\left(\Delta K_I\right)^4 + 8\left(\Delta K_{II}\right)^4 + \frac{8\left(\Delta K_{III}\right)^4}{1-\nu}\right]^{0.25} \tag{6}$$

The J-integral concept, originally proposed for correlation of crack growth rates under mode I, has also been extended to mixed-mode crack growth rate applications [44]. This approach was shown to correlate small crack growth rate data of Inconel 718 tubular specimens under axial, torsion, and proportional axial-torsion straining [44].

SUMMARY

The large amount of experimental data and research over the last four decades has significantly advanced the understanding of multiaxial fatigue. However, due to the challenging nature of the problem as well as its practical application significance, much additional research and development work is still needed for reliable multiaxial fatigue life estimation. This overview paper discussed several important issues related to multiaxial fatigue and some simple approximations for life estimations under multiaxial loads were presented.

As fatigue cracks nucleate and grow on preferred planes rather than with random orientation, understanding and capturing of the damage mechanisms is an essential requirement for proper life estimation modeling under multiaxial loads or stresses. Consequently, critical plane approaches which reflect the physical nature of fatigue damage process have been found to be most reliable and robust for multiaxial fatigue life estimations.

Some materials exhibit additional cyclic hardening under non-proportional loading conditions. This hardening is attributed to the change in crystallographic slip planes due to the rotation and intersection of maximum shear planes. The level of non-proportional hardening depends on the shape, sequence, and amplitude of the load path, as well as the microstructure of the material.

Sensitivity of a material to non-proportional cyclic loading is usually determined by non-proportional cyclic hardening coefficient. It has been found that cyclic hardening materials also exhibit non-proportional hardening under non-proportional loading, whereas cyclic softening materials do not typically display additional cyclic hardening. Therefore, the value of non-proportional cyclic hardening coefficient may be estimated based on uniaxial cyclic deformation properties, as presented.

Empirical formulations for predicting stress response in non-proportional loading based on strain path, although simple to use, may result in significant errors in estimated stresses and, therefore, fatigue life. Constitutive models requiring a small number of material constants can estimate the stress-strain response much more accurately.

Out-of-phase or non-proportional loading usually results in shorter fatigue life, compared to proportional loading. Although the shorter life is often attributed to non-proportional hardening, materials without this hardening also typically exhibit shorter life under such loading. Classical criteria, such as von Mises effective strain, cannot predict this behavior and should not be used for non-proportional loading.

Much work in the last 30 years suggests critical plane approaches are most reliable and robust for multiaxial fatigue life estimations. These approaches consider specific plane(s) with maximum fatigue damage as the critical plane and are, therefore, also able to predict damage (i.e. crack) orientation. Critical plane models with both stress and strain terms are the most appropriate due to their general applicability to both LCF and HCF, and for their ability to capture material constitutive response under non-proportional loading.

A difficulty in multiaxial life estimation is often lack of needed material fatigue properties. To enable calculation of multiaxial fatigue life in the absence of any fatigue

data, a simple approximation for steels based on hardness was presented. Estimated fatigue lives based on only hardness as material property were shown to compare favorably with experimental lives for several steels and under a wide variety of loading conditions.

In addition to a proper fatigue damage model, a cycle counting method to identify cycles in a load history, and a cumulative damage rule to sum damage from all the counted cycles are needed for evaluating fatigue life under variable amplitude multiaxial loading. Some of the shortcomings attributed to LDR in estimating fatigue lives in the literature are not necessarily due to LDR, but due to the use of an unsuitable damage parameter. In spite of the fact that LDR does not account for some of the load sequence and load path alteration effects, it can still result in reasonable life estimates if used with a proper damage parameter.

There are only a few proposals in the literature for cycle counting under multiaxial loading histories based on critical plane approaches. Developing a robust cycle counting method for variable amplitude loading remains a challenging problem in multiaxial fatigue.

Mixed-mode crack growth can constitute a significant portion of the total fatigue life. As the crack often changes direction during its growth under mixed-mode loading, both growth rate and growth direction are of importance. Maximum tangential stress and minimum strain energy density criteria have been widely used to predict crack growth direction because of their simplicity and support by experimental observations. Crack growth rates under mixed-mode loading have also been successfully correlated using equivalent strain intensity factors, as well as by extension of the J-integral.

REFERENCES

1. Lanza, G. (1886) *Transactions of the ASME* **8**: 130-144.
2. Gough, H.J. and Pollard, H.V. (1935) *Proc. Inst. Mech. Eng.* **131**: 3-103.
3. Gough, H.J. (1950) *J. Appl. Mech.* **50**: 113-125.
4. Sines, G. (1959) In: G. Sines and J.L. Waisman. (Eds.), *Metal Fatigue*, McGraw-Hill, New York, pp. 145-169.
5. Findley, W.N. (Nov. 1959) *J. Eng. Indus.* 301-306.
6. Socie, D.F. and Marquis, G.B. (2000) *Multiaxial Fatigue*, Society of Automotive Engineers.
7. Hua, C.T. and Socie, D.F. (1985) *Fatigue Eng. Mater. Struct.* **8**: 101-114.
8. Bannantine, J.A. and Socie, D.F. (1985) ASTM STP 942, 899-921.
9. Brown, M.W. and Miller, K.J. (1979) *Fatigue Eng. Mater. Struct.* **1**: 231-246.
10. Brown, M.W. and Miller, K.J. (1979) *Fatigue Eng. Mater. Struct.* **1**: 217-229.
11. Mars W. V. and Fatemi, A. (2006) *J. Mater. Sci.* **41**, 7324-7332.
12. Taira, S., Inoue, T., and Yoshida, S. (1968). *In: Proceedings of 11th Japan Congress on Mater. Res.*, pp. 60-65.
13. Lamba, H.S. and Sidebottom, O.M. (1978) *J. Eng. Mater. Technol.*, *Trans. ASME* **100**: 96-103.

14. Kanazawa, K., Miller, K.J., and Brown, M.W. (1979) *Fatigue Eng. Mater. Struct.* **2**: 217-228.
15. Shamsaei, N., Gladskyi, M., Panasovskyi, K., Shukaev, S., and Fatemi, A. (2010). Submitted to *Int. J. Fatigue*.
16. Shamsaei, N. and Fatemi, A. (2010). *Mater. Sci. Eng. A*. To appear.
17. Shamsaei, N., Fatemi, A., and Socie, D.F. (2010) *Int. J. Plast.* To appear.
18. Armstrong, P.J. and Frederick, C.O. (1966). *Report RD/B/N 731*, *Central Electricity Generating Board.*
19. Jiang, Y.Y., Kurath, P. (1996) *Int. J. Plast.* **12**: 387-415.
20. Chaboche, J.L. (2008) *Int. J. Plast.* **24**: 1642-1693.
21. Tanaka, E. (1994) *Eur. J. Mech. A. Solids.* **13**: 155-173.
22. Zhang, J.X. and Jiang, Y.Y. (2008) *Int. J. Plast.* **24**: 1890-1915.
23. Shamsaei, N., Fatemi, A., and Socie, D.F. (2010) *9th Int. Conf. Multiaxial Fatigue Fract.,* Parma-Italy.
24. Shamsaei, N. and Fatemi, A. (2009) *Fatigue Fract. Eng. Mater. Struct.* **32**: 631-646.
25. Mars W. V. and Fatemi, A. (2005) *Fatigue Fract. Eng. Mater. Struct.* **28**: 515-522.
26. Mars W. V. and Fatemi, A. (2005) *Fatigue Fract. Eng. Mater. Struct.* **28**: 523-538.
27. Findley, W.N. (1959) *J. Eng. Industry, Trans. ASME* **81**: 301.
28. Fatemi, A. and Socie, D.F. (1988) *Fatigue Fract. Eng. Mater. Struct.* **11**: 149-165.
29. Smith, R.N., Watson, P.P., and Topper, T.H. (1970) *J. Mater.* **5**: 767-778.
30. Fatemi, A. and Kurath, P.P. (1988) *J. Eng. Mater. Technol.*, *Trans. ASME* **110**: 380-388.
31. Roessle, M.L. and Fatemi, A. (2000) *Int. J. Fatigue* **22**: 495-511.
32. Fatemi, A. and Yang, L. (1998) *Int. J. Fatigue* **20**: 9-34.
33. Colin, J. and Fatemi, A. (2010) *Fatigue Fract. Eng. Mater. Struct.* doi: 10.1111/j.1460-2695.2009.01429.x
34. Miller, K.J. (1993) *J. Mater. Sci. Technol.* **9**: 453-462.
35. Harada, S. and Endo, T. (1991) European Structural Integrity Society, ESIS Publication 10, Mechanical Engineering Publications, London, pp. 161-178.
36. Harbour, R. J., Fatemi, A. and Mars W.V., (2008) *Int. J. Fatigue* **30**: 1231-1247.
37. Bannantine, J.A. and Socie, D.F. (1991). In: K. Kussmaul, D. McDiarmid, D. Socie (Eds.), *European Structural Integrity Society*, ESIS 10, MEP, London, pp. 35-51.
38. Wang, C.H. and Brown, M.W. (1996) *J. Eng. Mater. Technol.*, *Trans. ASME* **118**: 367-370.
39. Qian, J. and Fatemi, A. (1996) *Eng. Fract. Mech.* **55**: 969-990.
40. Erdogan, F. and Sih, G.C. (1963) *J. Bas. Eng., Trans. ASME* **85**: 519-525.
41. Sih, G.C. (1974) *Int. J. Fract.* **10**: 305-321.
42. Reddy, S.C. and Fatemi, A. (1992). In: M.R. Mitchell and R.W. Landgraf (Eds.) *Advances in Fatigue Lifetime Predictive Techniques*, ASTM STP 1122, Philadelphia, PA, pp. 569-585.
43. Tanaka, K. (1974) *Eng. Fract. Mech.* **6**: 493-507.
44. Hoshide, T. and Socie, D.F. (1987) *Eng. Fract. Mech.* **26**: 841-850.